

Supplemental Figures and Tables

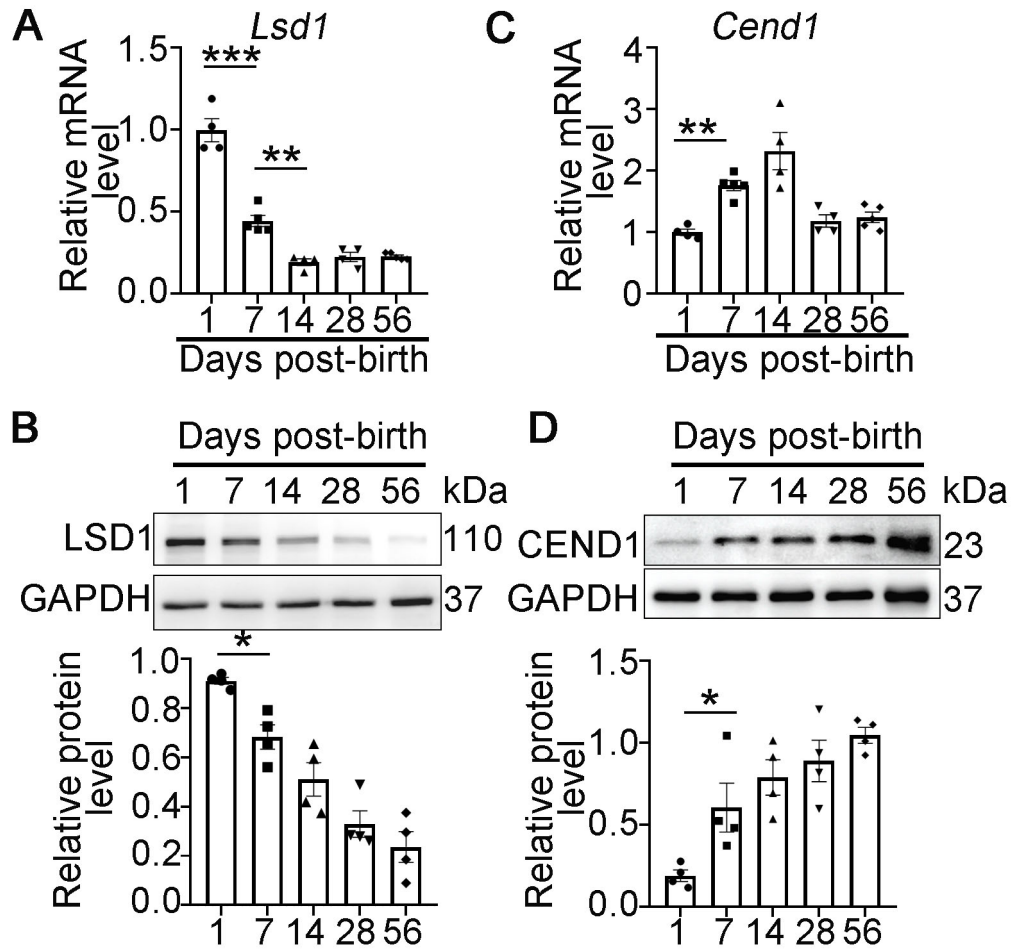


Figure S1. Complimentary expression of LSD1 and CEND1 in postnatal murine heart tissues. (A, C) qPCR analysis of *Lsd1* (A) and *Cend1* (C) mRNA levels in hearts of mice at indicated stages (n = 4-5/group). (B, D) Western blotting analysis of LSD1 (B) and CEND1 (D) protein levels in hearts of mice at indicated stages (n = 4/group).

* $p < 0.05$, ** $p < 0.01$, *** $p < 0.001$ by unpaired student's *t*-test.

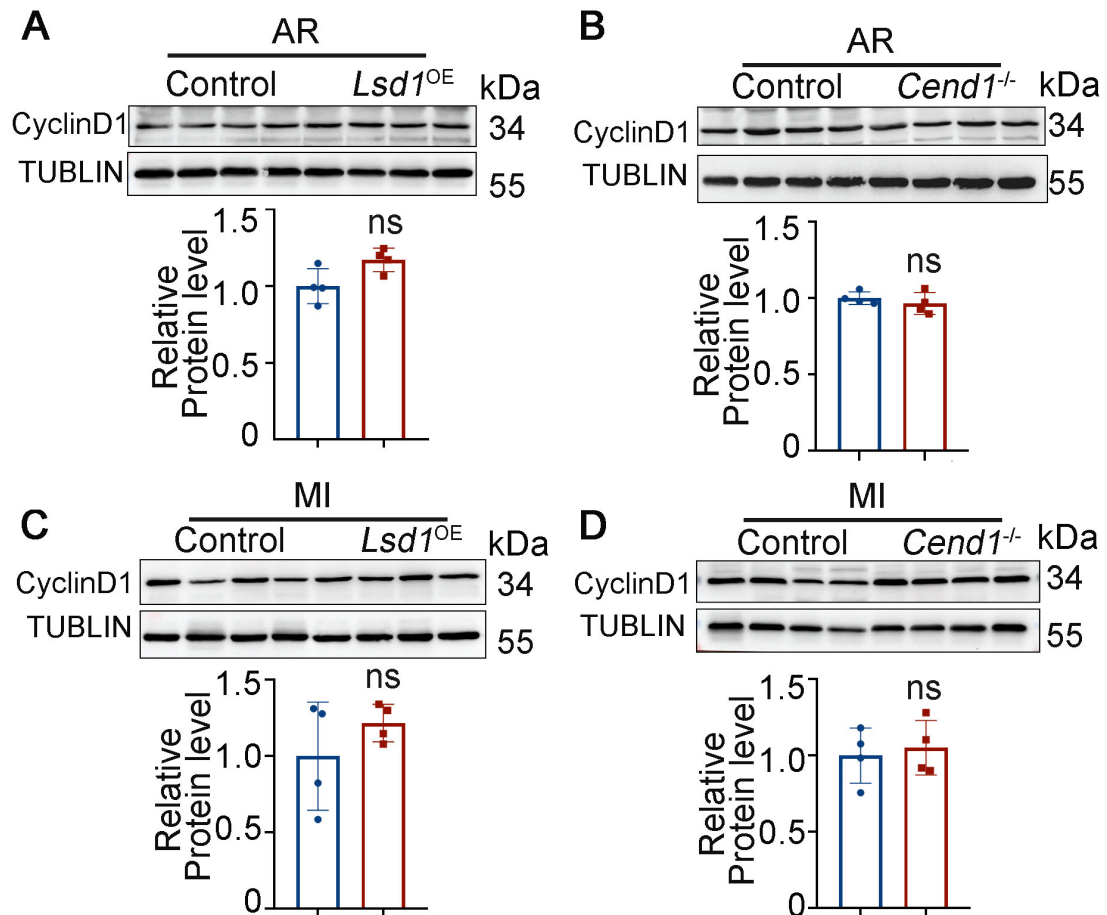


Figure S2. Cyclin D1 protein levels were unaffected by genetic manipulations of *Lsd1* or *Cend1* following heart injuries. (A-D) Western blotting analysis of CyclinD1 protein levels in the hearts of *Lsd1*^{OE} (A, C) and *Cend1*^{-/-} (B, D) mice following apical resection (AR) at neonatal stage (A, B) and myocardial infraction (MI) at adult stage (C, D). (n = 4/group). ns, no significance by unpaired student's *t*-test.

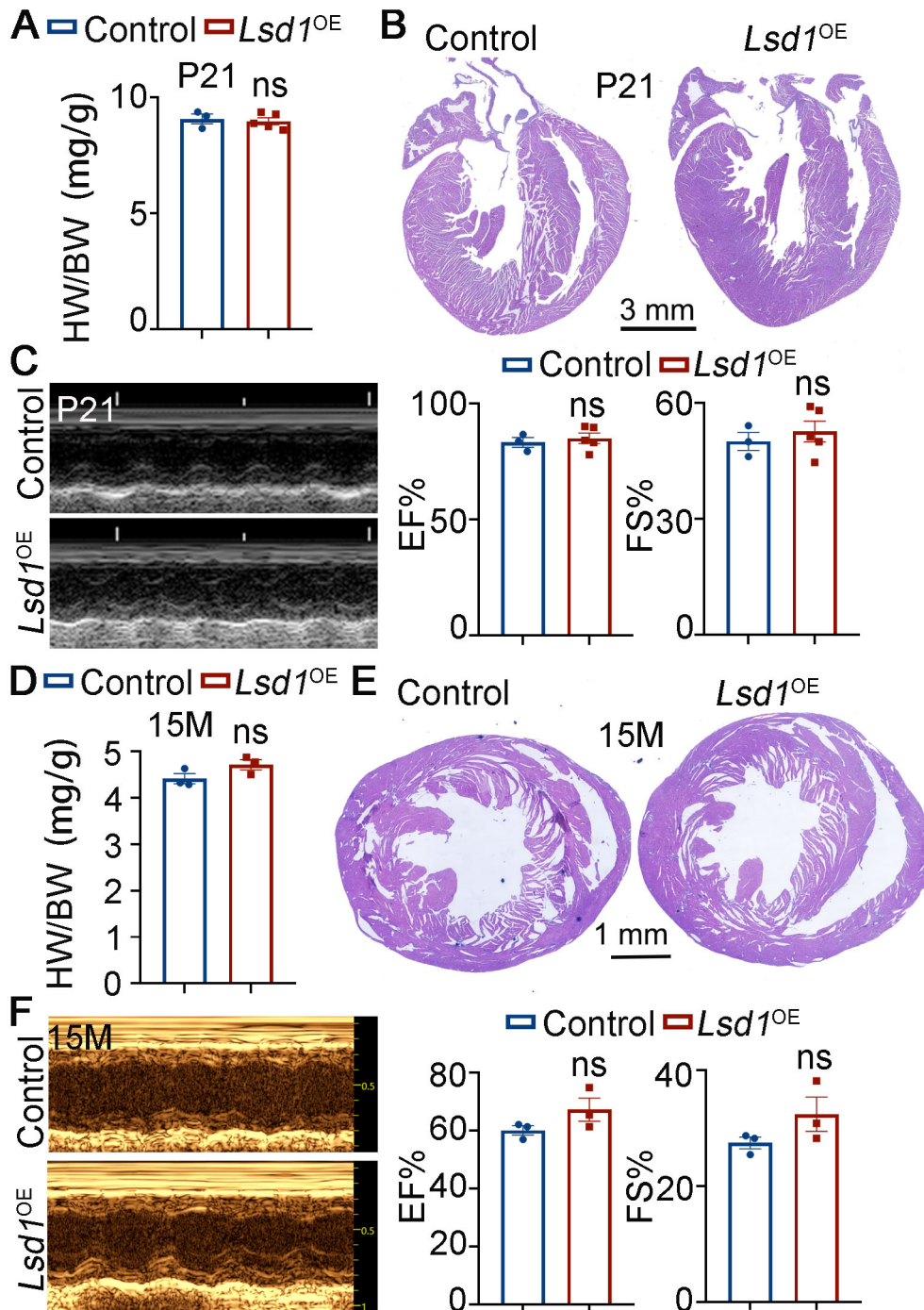


Figure S3. LSD1 overexpression does not alter cardiac structure or function in mice. (A) Heart weight-to-body weight (HW/BW) ratios in P21 $Lsd1^{OE}$ (n = 5) and control (n = 3) mice. (B) Representative hematoxylin and eosin (H&E)-stained heart sections from P21 mice. (C) Representative echocardiograms from P21 mice and quantification of ejection fraction (EF) and fractional shortening (FS) in control (n = 3) and $Lsd1^{OE}$ (n = 5) groups. (D) HW/BW ratios in 15-month-old (15 M) mice (n = 3/group). (E) H&E-stained heart sections from 15 M mice. (F) Representative echocardiograms from 15 M mice and quantification of EF and FS (n = 3/group). ns, no significance by unpaired student's *t*-test.

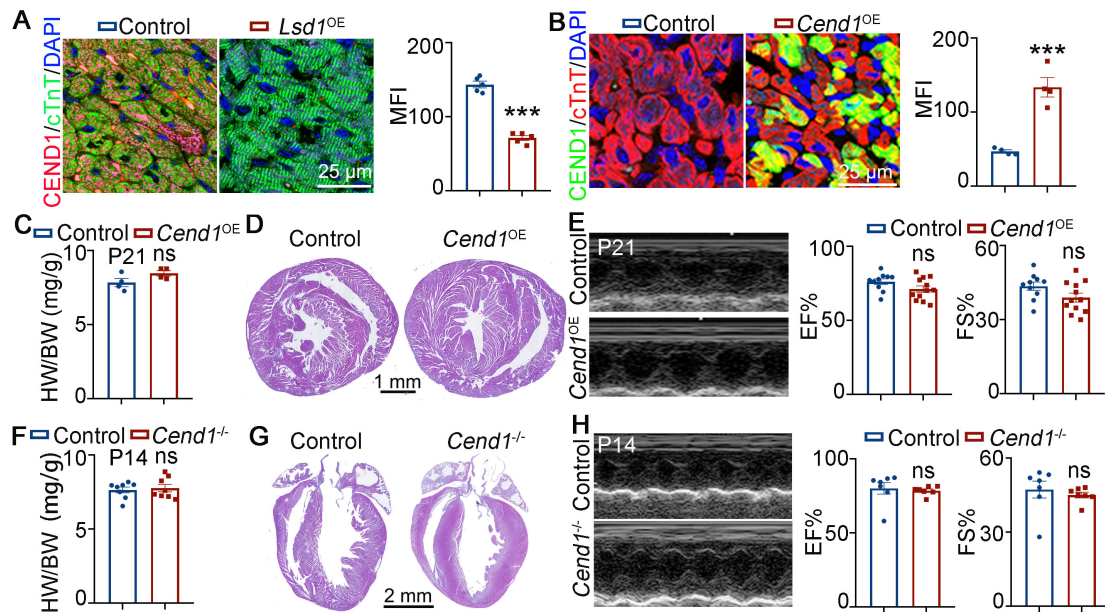


Figure S4. Cardiac structure and function are unaffected by *Cend1* genetic manipulation. (A) Co-immunostaining of CEND1 and cTNT antibodies in P14 *Lsd1^{OE}* and Control hearts (n = 5/group). The mean fluorescence intensity (MFI) was quantified and shown. (B) Co-immunostaining of CEND1 and cTNT antibodies in P14 *Cend1^{OE}* and Control hearts (n = 4/group). MFI was quantified and shown. (C) Heart weight-to-body weight (HW/BW) ratios in P21 mice (n = 4/group). (D) Representative H&E-stained heart sections from P21 mice. (E) Representative echocardiograms from P21 mice and quantifications of ejection fraction (EF) and fractional shortening (FS) in Control (n = 10) and *Cend1^{OE}* (n = 12) groups. (F) HW/BW ratios in P14 *Cend1^{-/-}* and Control mice (n = 8/group). (G) H&E-stained heart sections from P14 *Cend1^{-/-}* and Control mice. (H) Representative echocardiograms from P14 mice and quantifications of EF and FS in *Cend1^{-/-}* (n = 7) and Control (n = 7) groups. ns, no significance, *** $p < 0.001$ by unpaired Student's t-test.

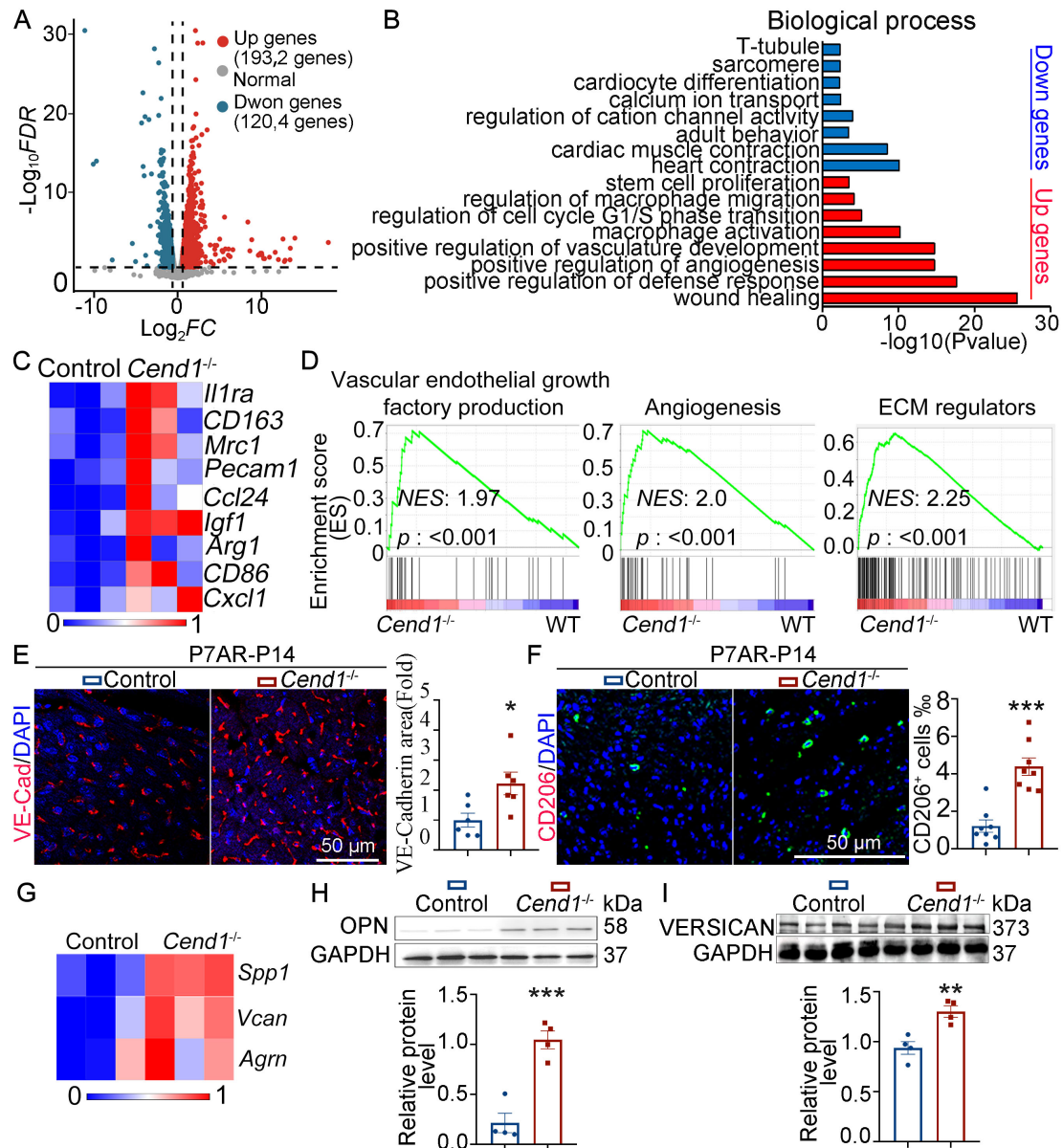


Figure S5. Loss of *Cend1* leads to gene expression alterations associated with cell proliferation, angiogenesis, and macrophage polarization. (A-D) Heart ventricle tissues were isolated from P14 control and *Cend1*^{-/-} mice which received apical resection (AR) surgeries at P7 and subjected to RNA-sequencing analysis. Volcano plots showing the differentially expressed genes (A). The chart showing the enriched biological processes revealed by Gene ontology (GO) analysis (B). A Heatmap showing the expression of M2 macrophage markers (C). The charts showing the enriched biological processes revealed by Gene Set Enrichment Analysis (GSEA) (D). (E) VE-cadherin immunostaining marking vascular endothelial cells within apex regions (n = 6/group). (F) Immunostaining for CD206 indicating M2 macrophages (n = 8/group). (G) Heatmap showing the expression of ECM genes (*Spp1*, *Vcan* and *Aggrn*) known to be involved in heart regeneration. (H, I) Western blotting analysis of OPN (encoded by *Spp1*) and Versican (encoded by *Vcan*) protein levels in P14 hearts (n = 4/group). ** $p < 0.01$, *** $p < 0.001$ by unpaired student's *t*-test.

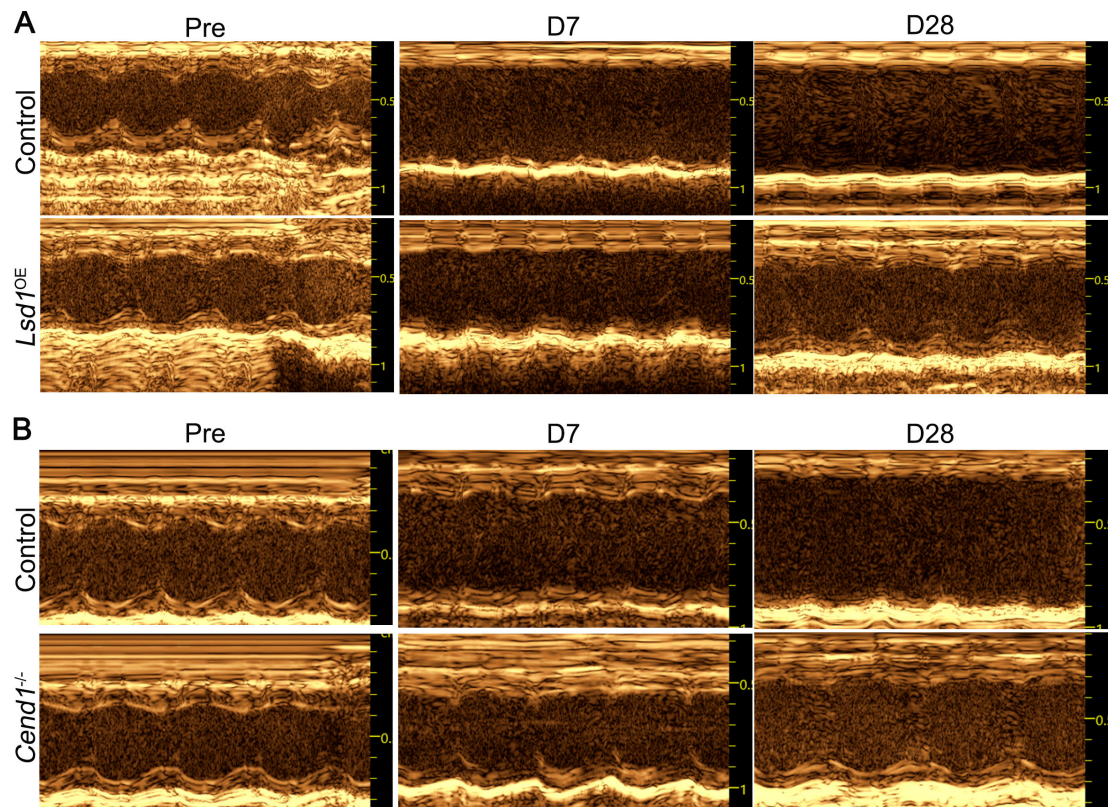


Figure S6. Echocardiographic assessment of cardiac function in *Lsd1^{OE}* and *Cend1^{-/-}* mice pre- and post-myocardial infarction (MI). Representative echocardiographic images of *Lsd1^{OE}* (A) and *Cend1^{-/-}* (B) mice at indicated time points. Pre, pre-MI; D7, Day 7 post-MI; D28, Day 28 post-MI.

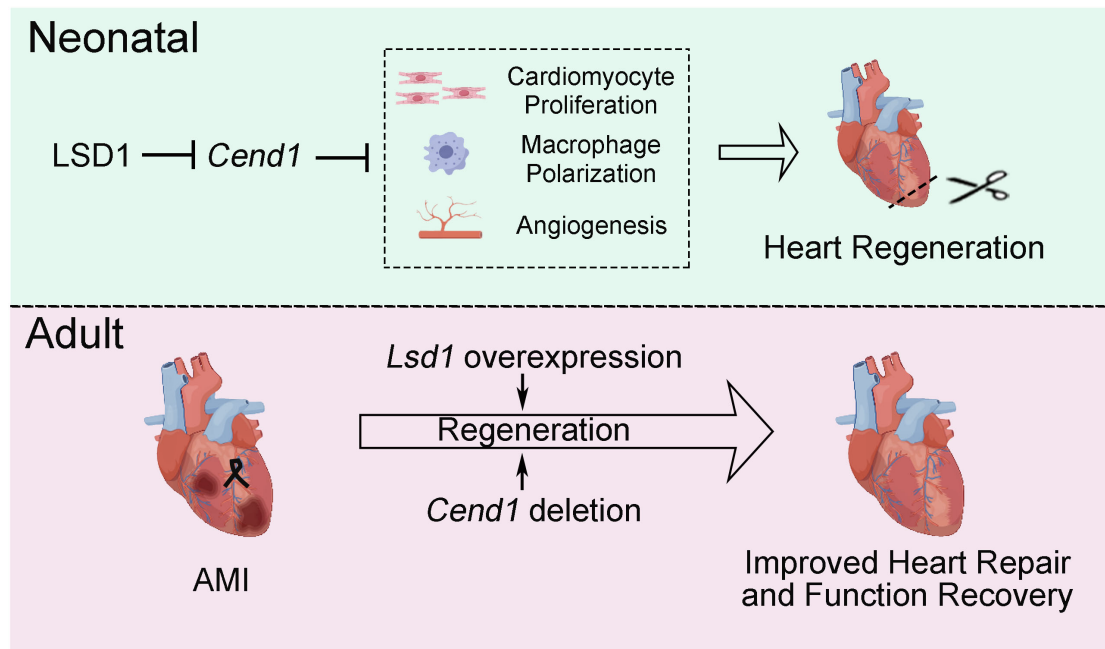


Figure S7. Diagrammatic summary for an LSD1-CEND1 signaling axis in neonatal and adult heart regeneration and repair. LSD1-dependent suppression of *Cend1* is essential for heart regeneration in neonatal mice. Mechanistically, *Cend1* negatively regulates cardiomyocyte proliferation, macrophage polarization and angiogenesis. Notably, both *Lsd1* overexpression and *Cend1* deletion can promote cardiac repair and functional recovery following myocardial infarction in adult mice, indicating that proper balanced achieved through regulation of a LSD1-CEND1 signaling axis may serve as therapeutic approach for heart disease in mammals.

Table S1. A list of antibodies used in this study.

Antibody	Company	Cat#	Source	WB dilution	IF dilution
AuroraB	abcam	ab2254	Rabbit	N/A	1:300
CEND1	CST	8944S	Rabbit	1:1000	1:200
cTnT	Proteintech	15513-1-AP	Rabbit	N/A	1:500
cTnT	Abcam	Ab8295	mouse	N/A	1:500
CyclinD1	Proteintech	60186-1-Ig	Mouse	1:3000	N/A
GAPDH	Proteintech	10494-1-AP	Rabbit	1:5000	N/A
Ki67	Abcam	ab15580	Rabbit	N/A	1:400
LSD1	CST	2139S	Rabbit	1:1000	1:200
OPN	CST	88742S	Rabbit	1:1000	N/A
PCNA	Abcam	Ab29	Mouse	1:1000	N/A
pH3	CST	9701S	Rabbit	N/A	1:400
VE-cadherin	R&D	AF1002	Goat	N/A	1:400
Versican	ABclonal	A19655	Rabbit	1:1000	N/A
α -Tublin	CST	2125S	Rabbit	1:1000	N/A

Table S2. A list of primers used in this study.

Mus gene	Forward sequence	Reverse sequence
<i>Lsd1</i>	CCAGGGATCGAGTAGGTGGA	GGAACAGCTTGTCCATTGGC
<i>Cend1</i>	GAAGACACCAGCCAAGGCAGAT	CTCCAGTGTGGACTCGTCCTC